A pentagonal bipyramidal cobalt(II) single-ion magnet tape

Meng-Tan Cai, [a#] Akshay Pratap Singh, [c#] Zi-Han Xu, [a] Dong Shao, *[a] Si-Chen Zhang, [a] Jiong Yang, [c] Bing-Shan Zhao, *[a,b] and Saurabh Kumar Singh *[c]

[a] *Hubei Key Laboratory of Processing and Application of Catalytic Materials, College of Chemistry and Chemical Engineering, Huanggang Normal University, Huanggang 438000, China*

[b] *Hubei Zhongke Industrial Technology Research Institute, Huanggang 438000, China*

[c] *Department of Chemistry, Indian Institute of Technology Hyderabad, Kandi-502285, Sangareddy, Telangana, India*

[d] *Department of Physics, Southern University of Science and Technology, Shenzhen 518055, China*

[#] *M.T.C. and A.P.S. contributed equally to this paper*

Correspondence and requests for materials should be addressed to

Email: shaodong@nju.edu.cn; zhaobingshan@hgnu.edu.cn; sksingh@chy.iith.ac.in

Table of Contents

EXPERIMENTAL SECTION

Materials and Synthesis. All reagents were purchased from commercially available sources and used without further purification. The ligands tpb was bought from TCI chemicals.

Synthesis of {[Co(TPB)(NO_3)$_2$]}$_n$ (Co). A mixture was prepared containing $Co(NO_3)_3 \cdot 6H_2O$ (23 mg, 0.05 mmol), TPB (30.9 mg, 0.1 mmol), DMF (1 mL), and water (7 mL). This mixture was then sealed in a 20 mL bottle and placed inside a microwave-assisted synthesis reactor. The reaction was heated at 80 °C under 3 barometric pressure for 8 hours. Following this heating period, a controlled cooling phase was initiated at a rate of 10 °C/h for 5 hours. Finally, the system was left to cool undisturbed to ambient temperature over a full day. This precise thermal regimen successfully yielded carmine block-shaped single crystals, which were obtained in a ca. 34% yield. Elemental analysis calcd. (%) for $C_{21}H_{15}CoN_5O_6$: C, 51.23; H, 3.07; N, 14.22. Found: C, 51.46, H, 3.11; N, 14.32. IR (KBr, cm^{-1}): 1773(vs), 1540(s), 1490(s), 1450(s), 1381(s), 1350(vs), 1260(s), 1028(w), 938(w), 736(vs), 693(s).

Physical measurements

Infrared spectra (IR) data were measured on KBr pellets using a Nexus 870 FT-IR spectrometer in the range of 4000-400 cm^{-1}. Elemental analyses of C, H, and N were performed at an Elementar Vario MICRO analyzer. Powder X-ray diffraction data (PXRD) were recorded on a Bruker D8 Advance diffractometer with Cu Kα X-ray source (λ = 1.54056 Å) operated at 40 kV and 40 mA. Thermal gravimetric analysis (TGA) was measured in Al_2O_3 crucibles using a PerkinElmer Thermal Analysis in the temperature range of 30-750 °C under an argon atmosphere. Magnetic measurements from 2 to 300 K with applied direct current (dc) field up to 7 T were performed using a Quantum Design SQUID VSM magnetometer on the crushed samples from the single crystals of the compound. Alternative current (ac) magnetic susceptibility data were collected in a zero-dc field or an applied 1000 Oe dc fields in the temperature range of 2-8 K, under an ac field of 2 Oe, oscillating at frequencies in the range of 1-1000 Hz. All magnetic data were corrected for the diamagnetic contributions of the sample holder and of core diamagnetism of the sample using Pascal's constants.

X-ray Crystallography

Single crystal X-ray diffraction data were collected on a Bruker D8 QUEST diffractometer with a PHOTON III area detector (Mo-Kα radiation, λ = 0.71073 Å, Bruker *Ius* 3.0) at 100 K. The APEX III program was used to determine the unit cell parameters and for data collection. The data were integrated and corrected for Lorentz and polarization effects using SAINT.[S1] Absorption corrections were applied with SADABS.[S2] The structures were solved by direct methods and refined by full-matrix least-squares method on *F*2 using the SHELXTL[S3] crystallographic software package integrated in Olex 2.[S4] All the non-hydrogen atoms were refined anisotropically. Hydrogen atoms of the organic ligands were refined as riding on the corresponding non-hydrogen atoms. Additional details of the data collections and structural refinement parameters are provided in Table 1. Selected bond lengths and angles were listed in Table S1 and S2. CCDC 2529850-2529851 are the supplementary crystallographic data for this paper. They can be obtained freely from the Cambridge Crystallographic Data Centre via www.ccdc.cam.ac.uk/data_request/cif.

Table S1. Structural and magnetic parameters of reported 1D coordination polymers showing SIM property.

Complex	Topology	symmetry	D (cm^{-1})	U_{eff} (K)	Ref.
$[Co(SCA)_2(MBIm)_2]_n$	Linear	T_d	−12.8(7)	11.3	6
$\{[Co_2(dmphen)_2(CPCA)_2]DMF\}_n$	Linear	D_{3h}	38.2(4)	9.2	7
$[Co(3\text{-}Hppt)_2(adip)(H_2O)_2]\cdot 2H_2O$	Linear	O_h	-33.9	29.08	8
$\{[Co(L1)(2,2'\text{-}bipy)]\cdot 0.5DMF\}_n$	Linear	D_{3h}	−56.2(2)	13.94	9
$\{[Co(bimb)(H_2O)_4]\cdot(L_2)\cdot 2DMF\}_n$	Linear	O_h	57.5(2)	8.82	9
$\{[Co(TPT)_{2/3}(H_2O)_4][CH_3COO]_2\cdot(H_2O)_4\}_n$	Linear	O_h	47.7	6.91	10
$[Co(L_{N3O2})]_6[Co^{III}(CN)_6]_4\cdot 26H_2O$	Linear	**D_{5h}**	21.4(6)	9.1	11
$[Co(tdmmb)(bpe)][BF_4]_2\cdot 3CH_3CN$	Linear	**D_{5h}**	21.7(7)	19.0	12
$[Co(btm)_2(SCN)_2\cdot H_2O]_n$	Linear	O_h	93.9	45.4	13
$\{[Mn^{III}(salen)(m\text{-}NC)_2Co^{III}(4,4\text{-}dmbipy)(CN)_2]\cdot H_2O\}_n$	Linear	O_h	-3.26	17.28	14
$\{[Mn^{III}(salen)(m\text{-}NC)_2Co^{III}(dmphen)(CN)_2]\}_n$	Linear	O_h	-4.38	13.54	15
$[Co(pytpy)(DClbdc)]_n$	Linear	O_h	-59.5	27.3	15
$[Co(pytpy)(ndc)]_n$	Zig-zag	O_h	-42.8	12.7	15
$[Co(btca)_{1/2}(mbpy)]_n$	Ribbon	D_{3h}	27.6	41.9	16
$\{[Co(HL)(EtOH)_2](ClO4)\}_n$	Linear	O_h	30.6	24.5	17
$\{[Co(H_3BTB)_2(phen)](NO_3)_2\}_n$	Linear	O_h	74.7	15.9	18
$[Co(pdms)(bpe)]_n$	Zig-zag	T_d	-21.1	77	19
$\{[Co(pdms)(tpb)]\cdot H_2O\cdot tpb\}_n$	Ribbon	T_d	-35.3	56.2	19
{[Co(pdms)(bpy)]·bpy}n	Zig-zag	T_d	-39.7	38.9	20
{[Co(pdms)(bpy)]·bpy}n	Zig-zag	T_d	-32.1	61.9	20
{[Co(pdms)(bpy)]·bpy}n	Zig-zag	T_d	-238	28.9	20
{[Co(pdms)(bpy)]·bpy}n	Zig-zag	T_d	-43.4	27.3	20
$\{[Co(TPB)(NO_3)_2]\}_n$	Ladder	**D_{5h}**			

Abbreviations: **SCA**, succinicacid; **MBIm**, 5,6-dimethylbenzimidazole; **dmphen**, 2,9-dimethyl phenanthroline; **H_2CPCA**, 3-(3-carboxyphenyl)-1H-pyrazole-5-carboxylic acid; 3-Hppt, 3-phenyl-5-(pyridin-3-yl)-1,2,4-triazole; **H_2adip**, adipic acid; **H_2L1**, 2,2'-[benzene-1,4-diylbis(methanediylsulfanediyl)]dibenzoic acid; **2,2'-bipy**, 2,2'-bipyridine; **H_2L2**, 2,2'-(1,4-phenylenebis(methylene))bis(sulfanediyl)dinicotinic acid; **bimb**, 1,4-bis(benzoimidazo-1-ly)benzene); **TPT**, 2,4,6-Tris(4-pyridyl)-1,3,5-triazine; **L_{N3O2}**, ligand derived from the and condensation of 2,6-diacetylpyridine with 3,6-dioxaoctane-1,8-diamine; **tdmmb**, 1,3,10,12-tetramethyl-1,2,11,12tetra-aza[3](2,6)pyridinoij3](2,9)-1,10-phenanthrolinophan-2,10-diene; **bpe**,

1,2diIJ4-pyridyl)ethane; btm, bis(1H-1,2,4triazol-1-yl)methane; **H_2salen**, N,N0-ethylenebis(salicylideneimine); **4,4-dmbipy**, 4,40-dimethyl-2,20-bipyridine; **dmphen**, 2,9-dimethyl-1,10-phenanthroline; H_4**btca** = 1,2,4,5-Benzenetetracarboxylic acid; **mbpy** = 4,4'-Dimethyl-2,2'-bipyridyl; H_2L = 2-{[(E)-1H-imidazol-4-ylmethylidene}amino]benzoic acid; H_3**BTB** = 1,3,5-tris(4-carboxylphenyl) benzene; **phen** = 1,10-phenanthroline; **bpy** = 4,4′-bipyridine, bpen = 1,2-di(4-pyridyl)ethylene; **bpdoz** = 2,5- di(pyridin-4-yl)-1,3,4oxadiazole; **bimp** = 1,4-bis[(1H-imidazol-1-yl)methyl]benzene; **H_2pdms** = 1,2-bis(methanesulfonamido)benzene, **bpe** = 1,2-di(4pyridyl)ethane; **tpb** = 1,2,4,5-tetra(4-pyridyl)benzene; **TPB** = 1,3,5-Tri(pyridin-4-yl)benzene.

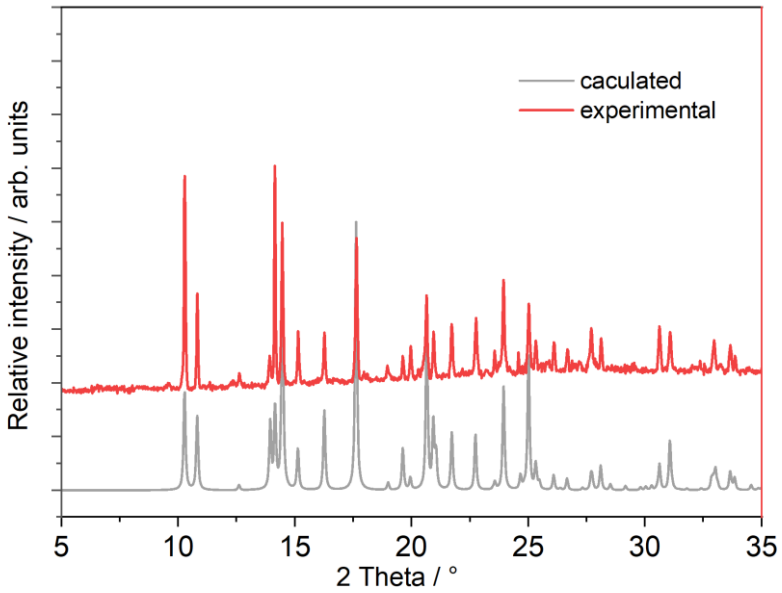

Figure S1. PXRD profiles of as-synthesized **Co**.

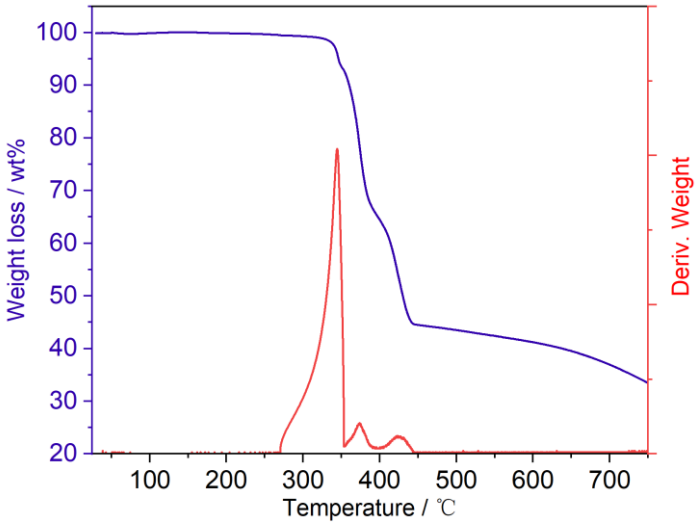

Figure S2. TGA of **Co**.

Table S2. Crystallographic data and structure refinement parameters for **Co**.

Temperature / K	300.00	400.00
Formula	$C_{21}H_{15}CoN_5O_6$	
Weight [g mol^{-1}]	492.31	
Crystal system	monoclinic	
Space group	C2/c	
a [Å]	11.5665(9)	11.680(2)
b [Å]	14.0305(9)	14.068(3)
c [Å]	13.2812(11)	13.278(2)
α [°]	90	90
β [°]	109.648(4)	109.880(6)
γ [°]	90	90
V [Å^3]	2029.8(3)	2051.6(7)
Z	4	4
ρ_{calcd} [g cm^{-3}]	1.611	1.581
μ(Mo–K_α) [mm^{-1}]	0.897	0.885
F (000)	1004.0	996.0
R_{int}	0.0453	0.0584
R_1 [a] / wR_2 [b] (I > 2σ(I))	0.0281 / 0.0664	0.0347 / 0.0928
R_1/ wR_2 (all data)	0.0331 / 0.0687	0.0415 / 0.0971
GOF on F^2	1.077	1.045
Max/min [e Å^{-3}]	0.29 / -0.22	0.45 / -0.25

[a] $R_1 = \sum||F_o| - |F_c||/\sum|F_o|$. [b] $wR_2 = \{\sum[w(F_o^2 - F_c^2)^2]/\sum[w(F_o^2)^2]\}^{1/2}$

Table S3. Selected bond lengths (Å) in **Co**.

T / K	300
Co1-O1	2.2953(15)
Co1-O1[1]	2.2953(15)
Co1-O2[1]	2.1842(16)
Co1-O2	2.1842(16)
Co1-N2[2]	2.1781(12)
Co1-N2[3]	2.1781(12)
Co1-N1	2.1416(18)
Co-N/$O_{average}$	2.2081
[1]1-X,+Y,3/2-Z; [2]1/2-X,1/2-Y,1-Z; [3]1/2+X,1/2-Y,1/2+Z	

Table S4. Selected bond angles (Å) in **Co**.

T / K	300
O1[1]-Co1-O1	174.60(7)
O2[1]-Co1-O1	129.63(5)
O2[1]- Co 1-O1[1]	55.75(5)
O2- Co1-O1	55.75(5)
O2[1]- Co1-O2	74.27(8)
N2[3]- Co1-O1	90.11(5)
N2[3]- Co1-N2[2]	170.80(7)
N1-Co1-O1[1]	87.30(3)
N1-N1-O2[1]	142.86(4)
N3-O2-Co1	97.89(11)
[1]1-X,+Y,3/2-Z; [2]1/2-X,1/2-Y,1-Z; [3]1/2+X,1/2-Y,1/2+Z	

Table S5. Continuous Shape Measure [S5] analysis for seven-coordinated Co^{II} centers in **Co.**

Metal center	HP-6	CShM value		coordination geometry
		300 K	400 K	
Co^{II}	Heptagon	34.292	34.272	Pentagonal bipyramid
	Hexagonal pyramid	21.544	21.298	
	Pentagonal bipyramid	**2.217**	**2.530**	
	Capped octahedron	6.883	6.941	
	Capped trigonal prism	4.980	5.029	
	Johnson pentagonal	5.638	6.053	
	Elongated triangular	21.386	21.034	

Table S6. Selected bond lengths (Å) in **Co**.

T / K	400
Co1-O1	2.277(2)
Co1-O1^{3}	2.277(2)
Co1-O2^{3}	2.197(3)
Co1-O2	2.197(3)
Co1-N2^{1}	2.1826(17)
Co1-N2^{2}	2.1826(17)
Co1-N1	2.134(2)
Co-N/O$_{average}$	2.2064
^{1}1/2+X,1/2-Y,1/2+Z; ^{2}1/2-X,1/2-Y,1-Z; ^{3}1-X,+Y,3/2-Z	

Table S7. Selected bond angles (Å) in **Co**.

T / K	400
N2^{1}-Co1-N2^{2}	171.17(9)
N2^{2}-Co1-O1^{3}	90.62(8)
N2^{2}-Co1-O1	89.23(8)
N2^{1}- Co1-O2	97.27(9)
O1- Co1-O1^{3}	178.07(10)
O2- Co1-O1^{3}	127.35(8)
O2^{3}- Co1-O1^{3}	54.58(8)
O2^{3}-Co1-O1	127.34(8)
N1-N1-O2	143.42(6)
N3-O1-Co1	94.41(16)
^{1}1/2+X,1/2-Y,1/2+Z; ^{2}1/2-X,1/2-Y,1-Z; ^{3}1-X,+Y,3/2-Z	

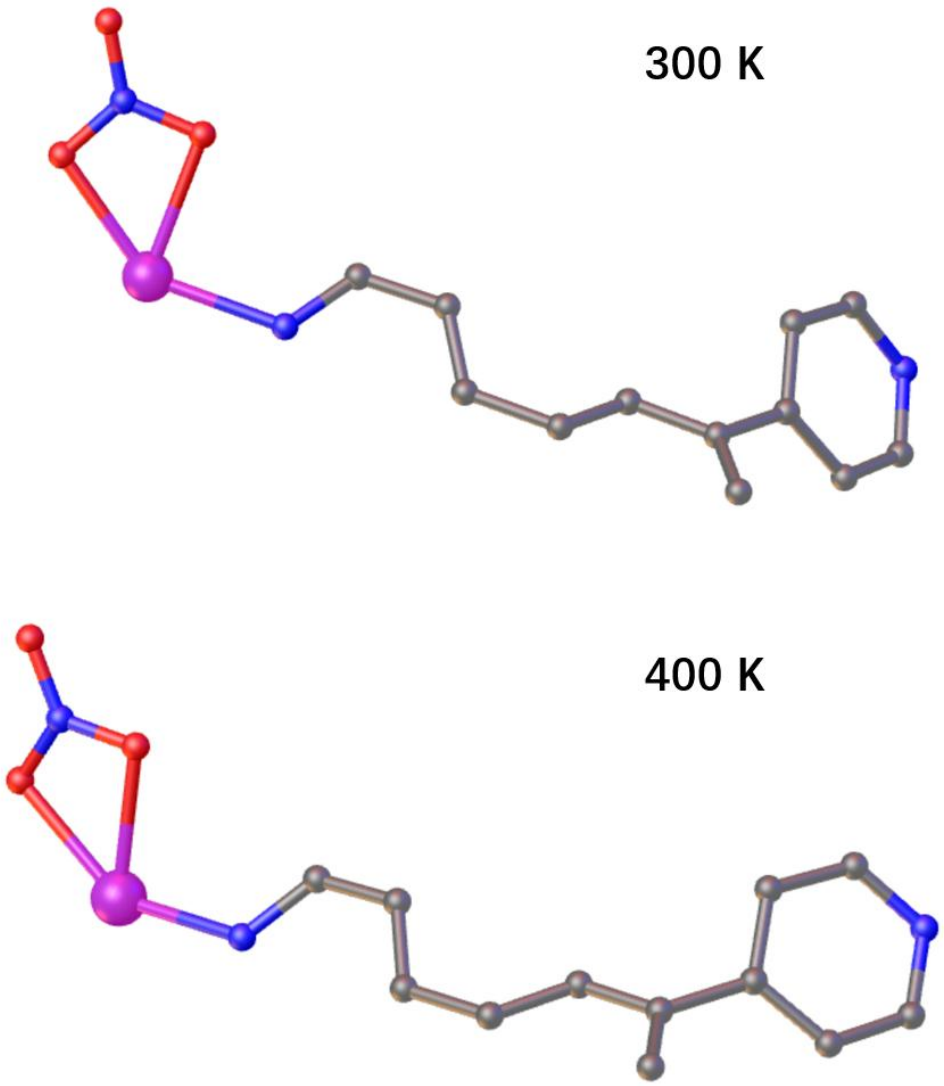

Figure S3. The asymmetric units of **Co** at 300 (up) and 400 K (down). Color code: C, black; O, red; N, blue; S, yellow; Co, purplish red. H atoms have been omitted for clarity.

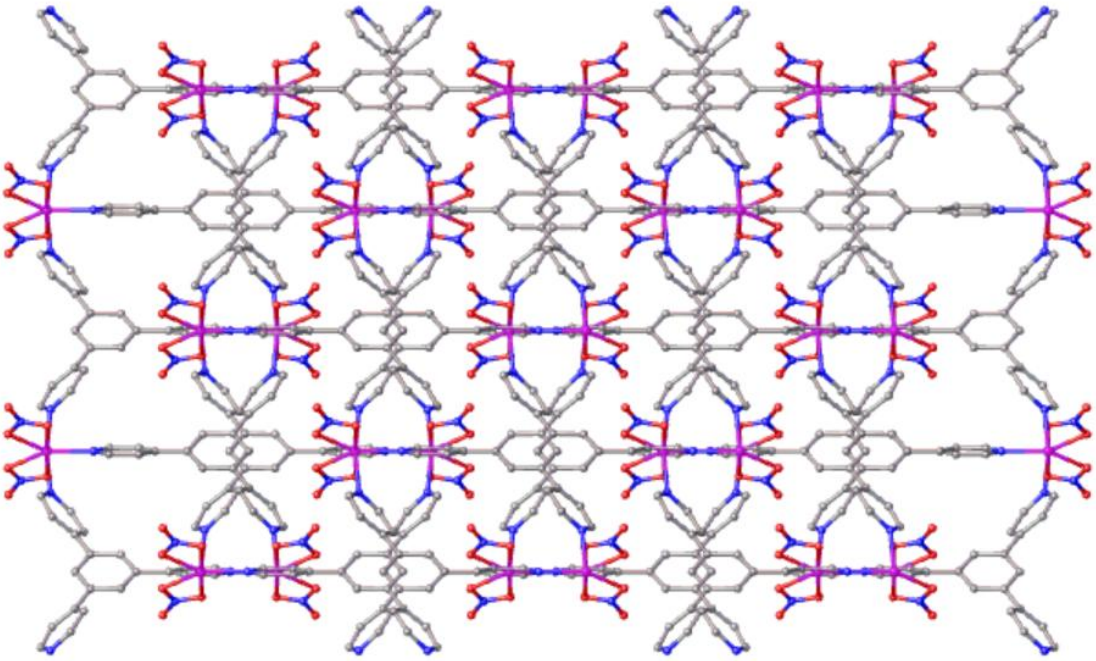

Figure S4. A portion of packing crystal structure of **Co** along *a* axis.

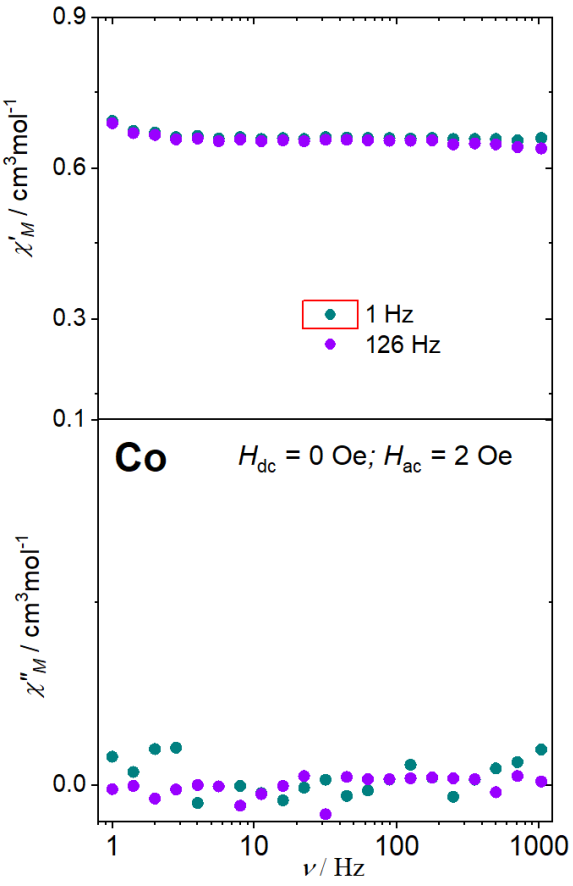

Figure S5. Frequency dependence of the ac susceptibilities measured under 0 Oe dc field for **Co**.

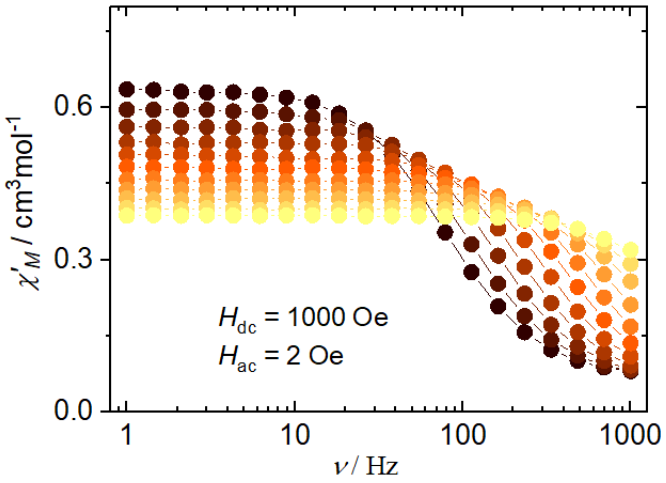

Figure S6. Frequency dependence of the in-phase (χ') part of the ac susceptibilities measured under 1 kOe dc field for **Co**.

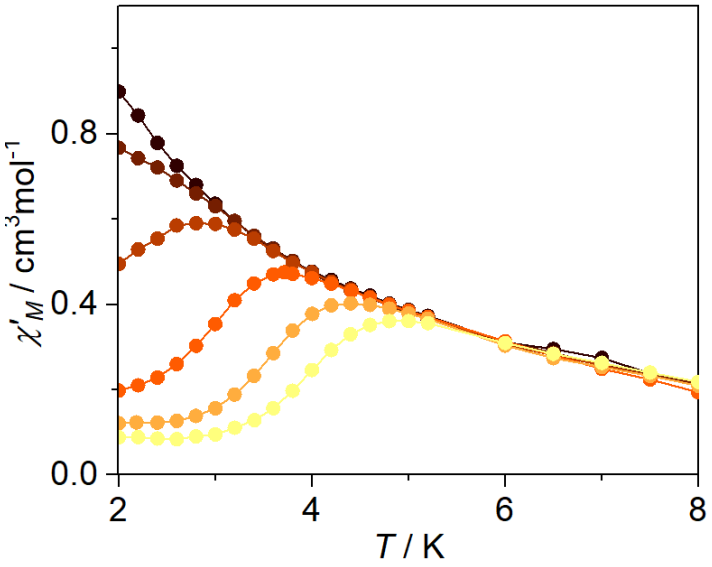

Figure S7. Temperature dependence of the in-phase (χ') and out-of-phase (χ'') part of the ac susceptibilities measured under 1 kOe dc field for **Co**.

Table S8. Relaxation fitting parameters from the least-square fitting of the Cole-Cole plots of **Co** under 1000 Oe dc filed according to the generalized Debye model.

T / K	τ / s	χ_S / $cm^3mol^{-1}K$	χ_T / $cm^3mol^{-1}K$	α
1.8	0.00105	0.0676	0.6489	0.07503
2.0	7.19472E-4	0.0628	0.6105	0.0603
2.2	4.89496E-4	0.0611	0.573	0.04515
2.4	3.40046E-4	0.0622	0.5423	0.03525
2.6	2.34653E-4	0.0590	0.514	0.04006
2.8	1.6361E-4	0.0561	0.4905	0.02073
3.0	1.15971E-4	0.0554	0.4663	0.03021
3.2	8.06235E-5	0.0463	0.4469	0.02511

Computational Details

All calculations were performed using the ORCA 5.0.3 code.[S21] Hydrogen-optimisation calculations were carried out at the BP86 level of theory [S22] using the SV basis sets for all atoms.[S23] Hydrogen-optimised coordinates have been taken further to calculate Spin-Hamiltonian (SH) parameters.

CASSCF calculation:

We compute the spin Hamiltonian, electronic and magnetic properties of individual Co (II) centres in model complex **Coa.** Complete active space self-consistent (CASSCF) calculations [S24,25] with an active space of CAS (7, 5), i.e., seven active electrons in the five active d-orbitals of Co (II). DKH approximation was used to incorporate scalar relativistic effects, and the DKH-adapted version of the DKH-def2-TZVP was used for the Co atom. In contrast, the def2-SVP basis set was used for the remaining atoms. Using an active space of CAS (7,5), we computed 10 quartets and 40 doublet states. Dynamic correlations were incorporated by second-order N-electron valence perturbation theory (NEVPT2) calculation,[S26-28] which was performed on top of the converged CASSCF wavefunctions. Further, ab-initio based ligand field theory (AILFT) analysis was used for the analysis of ligand field and d-orbital splitting as implemented in ORCA.

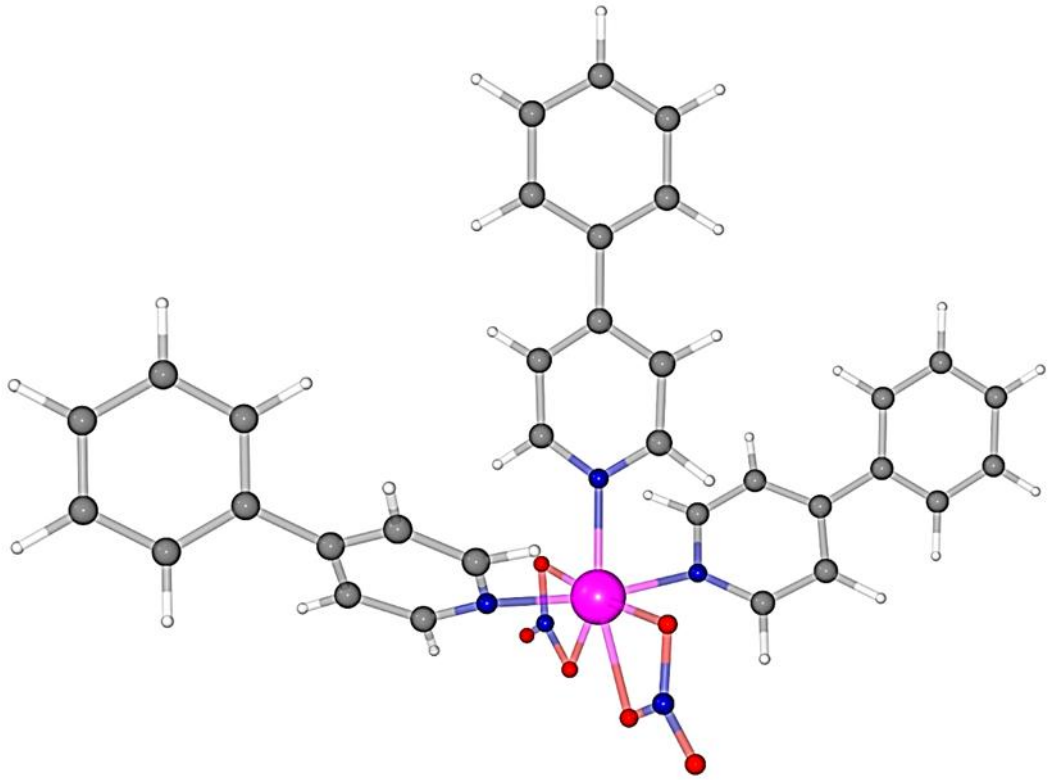

Figure S8. Hydrogen optimized structure of model complex **Coa**. The position of hydrogen was optimized using DFT calculations. Colour code: pink, Co; dark blue, N; red, O; grey, C; white, H.

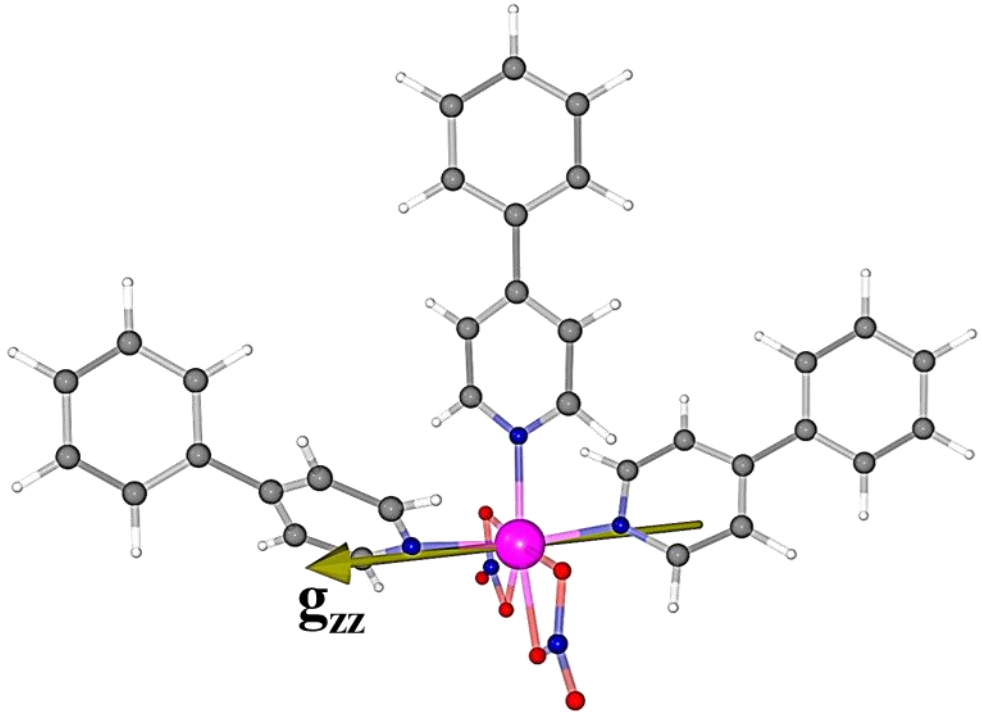

Figure S9. NEVPT2 computed the orientation of the g_{zz} axes in model complex **Coa**. Colour code: pink, Co; dark blue, N; red, O; grey, C; white, H.

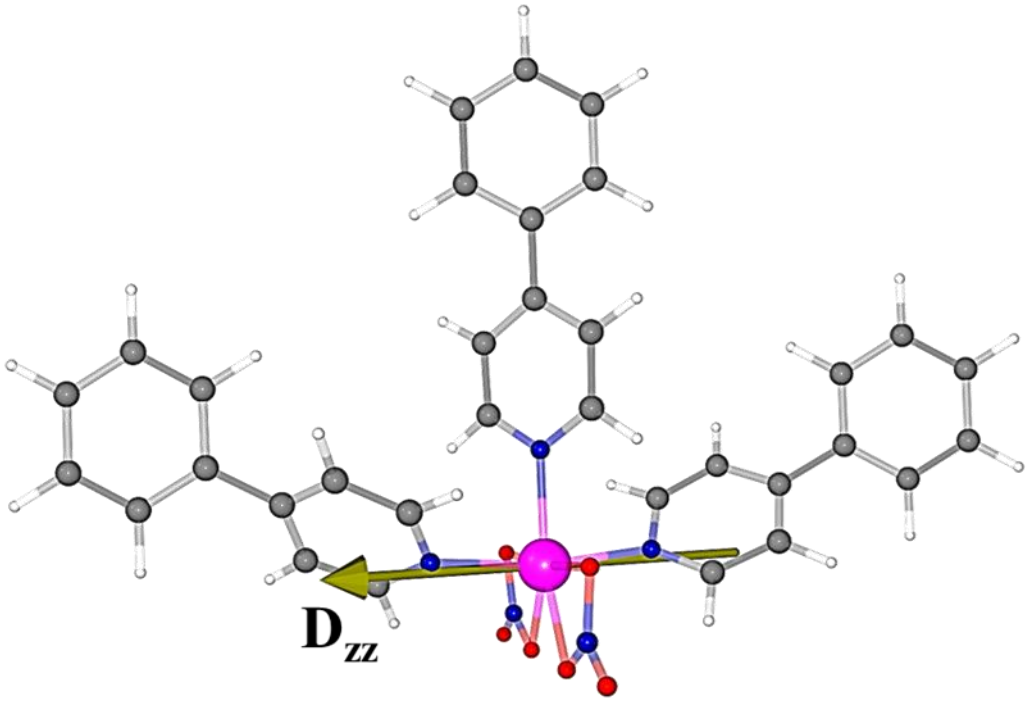

Figure S10. NEVPT2 computed the orientation of the D_{zz} axes in model complex **Coa**. Colour code: pink, Co; dark blue, N; red, O; grey, C; white, H.

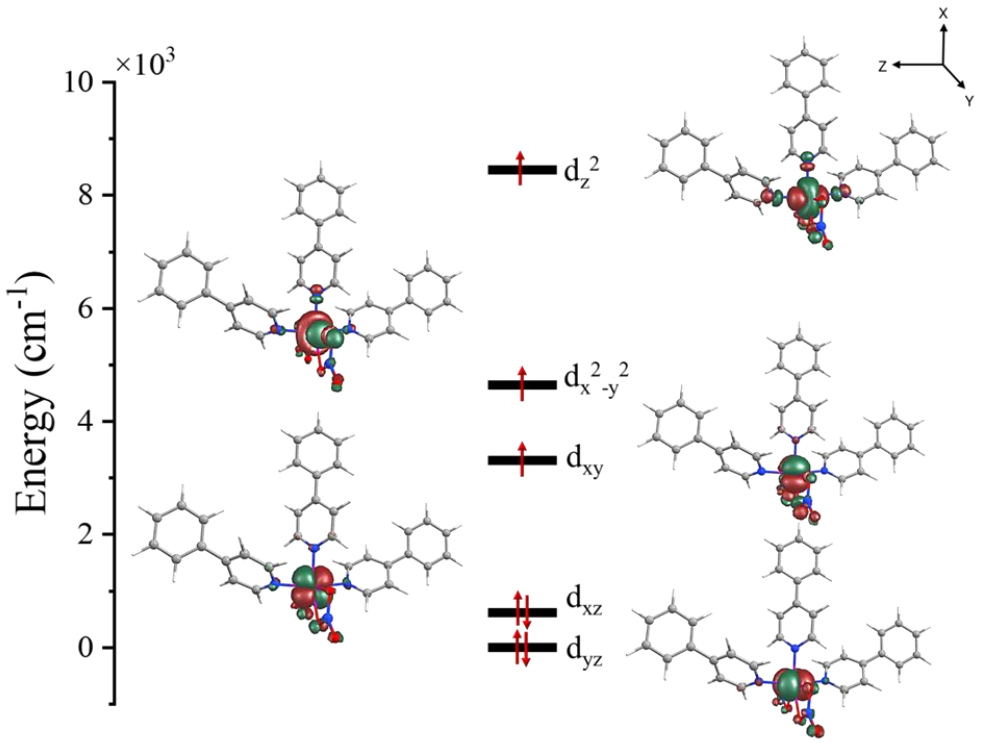

Figure S11. NEVPT2 - ab initio ligand field theory (AILFT) computed ordering of the d-orbital for model complex **Coa.**

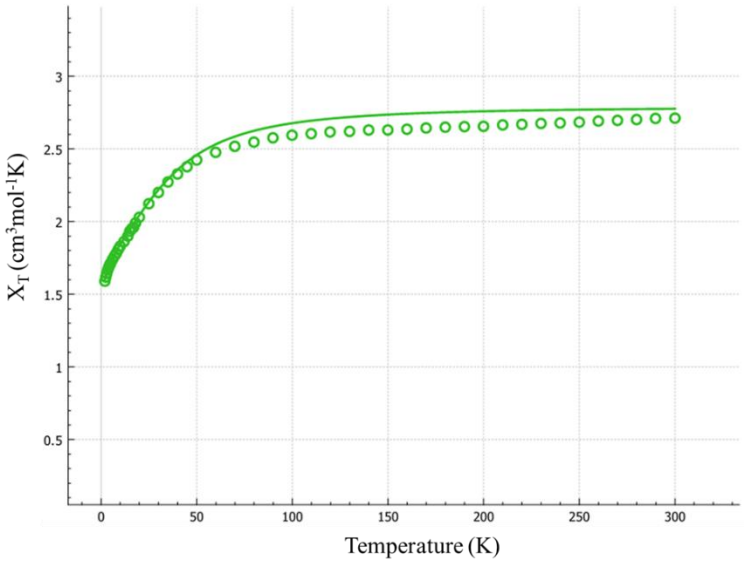

Figure S12. DFT simulated magnetic susceptibility plot for model complex **Coa**. The circles represent the experimental values, while the solid line represents the simulated data.

Table S9. CASSCF (7,5) + NEVPT2 computed Spin-Hamiltonian parameters (g, D, |E/D| parameters) along with wavefunction decomposition analysis of model complex **Coa**.

Complex	**Coa**	
Parameters	**NEVPT2**	**CASSCF**
D (cm^{-1})	37.28	44.83
|E/D|	0.195	0.225
g_{xx}	2.022	2.027
g_{yy}	2.285	2.361
g_{zz}	2.440	2.578
KD1 $\|\pm m_s\rangle$	56% |±3/2>	54% |±3/2>

g_{xx}	1.807	1.743
g_{yy}	3.183	3.066
g_{zz}	6.095	6.591
KD2 $\|\pm m_s\rangle$	56% |±3/2>	54% |±3/2>
g_{xx}	1.223	1.454
g_{yy}	1.390	1.663
g_{zz}	5.857	5.806

Table S10. Energies (in cm^{-1}) of spin-free ground and first four excited states of the *S* = 3/2 states spanned by the d^7 configuration in model complex **Coa** and the constituting electronic configurations.

Root	Energy (cm^{-1})	Electronic Configuration
0	0	$0.69\ (d_{z^2})^1 (d_{yz})^2 (d_{x^2-y^2})^1 (d_{xy})^1 (d_{xz})^2$
1	3217	$0.64\ (d_{z^2})^2 (d_{yz})^2 (d_{x^2-y^2})^1 (d_{xy})^1 (d_{xz})^1$
2	3284	$0.74\ (d_{z^2})^2 (d_{yz})^1 (d_{x^2-y^2})^2 (d_{xy})^1 (d_{xz})^2$
3	4953	$0.49\ (d_{z^2})^1 (d_{yz})^1 (d_{x^2-y^2})^1 (d_{xy})^2 (d_{xz})^2$
4	6370	$0.88\ (d_{z^2})^1 (d_{yz})^2 (d_{x^2-y^2})^2 (d_{xy})^1 (d_{xz})^1$

Table S11. Energies (in cm^{-1}) of spin-free ground and first four excited states of the *S* = 3/2 states spanned by the d^7 configuration in model complex **Coa** and the constituting electronic configurations.

Root	**Contribution to D (cm^{-1})**	
	NEVPT2	**CASSCF**
1	8	11
2	0.4	1
3	13	18
4	11	13

Table S12. CASSCF/NEVPT2 computed 10 spin-free quartets (red) and 40 spin-free doublets (blue) states, along with spin-orbit states for model complex **Coa**. All the values are reported here in cm^{-1}.

SPIN-FREE STATES				**SPIN-ORBIT STATES**			
CASSCF		**NEVPT2**		**CASSCF**		**NEVPT2**	
0	30192.2	0	29431.5	0	26473.89	0	24305.55
2283.2	30510.3	3216.7	30309.8	0	26473.89	0	24305.55
2315.1	30913.4	3283.9	30915.6	96.26	27215.91	78.68	24920.92
3668.5	31150.6	4953.1	31214.7	96.26	27215.91	78.68	24920.92
4908.8	31328.1	6369.7	31315.7	1824.3	28214.21	2740.46	27349.73
8996.6	31726.7	11795.3	31905.7	1824.3	28214.21	2740.46	27349.73
10872.2	31810.6	14175.4	32184.8	2261.72	28303.7	3173.68	27467.19
22186.5	32897.7	20737.7	32728.1	2261.72	28303.7	3173.68	27467.19
23427.6	33358.2	22450.6	33503.8	2634.72	29874.09	3548.79	29098.95
24512.6	33768.6	23333.5	33686	2634.72	29874.09	3548.79	29098.95
16927.9	34069	13882.3	33686.4	2877.75	30382.49	3817.35	29697.13
18368.4	34449.6	15887.5	34735	2877.75	30382.49	3817.35	29697.13
19704.5	35267.1	17716.3	35693.8	3861.39	30742.03	5095.67	30511.49
20274.8	46777.6	18751.5	42538.5	3861.39	30742.03	5095.67	30511.49
21439.1	46993.4	20862.3	43134.7	4014.64	31013.87	5220.73	30960.15

21512.8	47548	21041.8	43917.4	4014.64	31013.87	5220.73	30960.15
21878.1	47793.1	21574.3	43962.7	5064.53	31417.02	6484.3	31178.66
22234.8	48037.7	21647.8	44329.9	5064.53	31417.02	6484.3	31178.66
22529.9	48277.6	21899.6	44580.4	5162.52	31698.12	6562.56	31639.47
25728	48436.8	22780.5	44786.4	5162.52	31698.12	6562.56	31639.47
25873.9	71296.9	23759.4	63877.4	9036.67	31739.59	11807.23	32132.52
26903.6	71649.1	24560.8	64307.3	9036.67	31739.59	11807.23	32132.52
28077.3	72639.9	27241	65212.2	9211.48	32300.3	11949.7	32469.86
28110.3	73194.6	27298.7	65792.6	9211.48	32300.3	11949.7	32469.86
29814.3	73756.9	29055.8	66643.5	11113.41	33143.38	13962.34	32997.53
				11113.41	33143.38	13962.34	32997.53
				11198.27	33584.7	14345.48	33440.54
				11198.27	33584.7	14345.48	33440.54
				16987.41	33891.45	14417.69	33916.87
				16987.41	33891.45	14417.69	33916.87
				18633.76	34284.48	16122.55	34019.03
				18633.76	34284.48	16122.55	34019.03
				19816.53	34829.64	17824.21	35043.19
				19816.53	34829.64	17824.21	35043.19
				20342	35814.15	18835.58	36101.89
				20342	35814.15	18835.58	36101.89
				21544.38	46927.25	20687.34	42666.62
				21544.38	46927.25	20687.34	42666.62
				21663.01	47154.81	20796.24	43264.17
				21663.01	47154.81	20796.24	43264.17
				22180.78	47709.2	20928.74	43982.84
				22180.78	47709.2	20928.74	43982.84
				22254.82	48025.07	21117.54	44210.98
				22254.82	48025.07	21117.54	44210.98
				22288.24	48189.89	21721.94	44440.13

				22288.24	48189.89	21721.94	44440.13
				22453.73	48516.98	21819.02	44783.73
				22453.73	48516.98	21819.02	44783.73
				22774.19	48696.45	22129.58	45001.84
				22774.19	48696.45	22129.58	45001.84
				23448.33	71479.83	22332.26	64032.69
				23448.33	71479.83	22332.26	64032.69
				23543.76	71872.57	22474.89	64492.14
				23543.76	71872.57	22474.89	64492.14
				24459.65	72845.46	22801.93	65389.41
				24459.65	72845.46	22801.93	65389.41
				24679.09	73420.51	23388.85	65996.75
				24679.09	73420.51	23388.85	65996.75
				25903.66	74019.8	23748.58	66860.77
				25903.66	74019.8	23748.58	66860.77

References

1) SAINT Software Users Guide, version 7.0; Bruker Analytical X-Ray Systems: Madison, WI, 1999.
2) G. M. Sheldrick, SADABS, version 2.03; Bruker Analytical X-Ray Systems, Madison, WI, 2000.
3) G. M. Sheldrick, SHELXTL, Version 6.14, Bruker AXS, Inc.; Madison, WI 2000-2003.
4) Dolomanov, O. V.; Bourhis, L. J.; Gildea, R. J.; Howard, J. A. K.; Puschmann, H. OLEX2: A Complete Structure Solution, Refinement and Analysis Program. *J. Appl. Crystallogr*., 2009, 42, 339−341.
5) M. Llunell, D. Casanova, J. Cirera, P. Alemany and S. Alvarez, SHAPE, Version 2.1. Universitat de Barcelona, 2013.
6) J.-J. Kong, D. Shao, C.-L. Ji, Y.-X. Jiang and X.-C. Huang, *CrystEngComm*, 2019, **21**, 749–757.
7) M. Roy, A. Adhikary, A. K. Mondal and R. Mondal, *ACS Omega.*, 2018, **3**, 15315−15324.
8) X. Liu, X. Ma, P. Cen, F. An, Z. Wang, W. Song and Y.-Q. Zhang, *New J. Chem*., 2018, **42**, 9612-9619.
9) Z. Chen, L. Yin, X. Mi, S. Wang, F. Cao, Z. Wang, Y. Li, J. Lua and J. Dou, *Inorg. Chem. Front*., 2018, **5**, 2314–2320.
10) D. Shao, L. Shi, H.-Y. Wei and X.-Y. Wang, *Inorganics*, 2017, **5**, 90.
11) D. Shao, L. Shi, F.-X. Shen and X.-Y. Wang, *CrystEngComm*, 2017, **19**, 5707–5711.
12) D. Shao, L. Shi, S.-L. Zhang, X.-H. Zhao, D.-Q. Wu, X.-Q. Wei and X.-Y. Wang, *CrystEngComm*, 2016, **18**, 4150–4157.
13) Y.-Y. Zhu, M.-S. Zhu, T.-T. Yin, Y.-S. Meng, Z.-Q. Wu, Y.-Q. Zhang and S. Gao, *Inorg. Chem*., 2015, **54**, 3716−3718.

14) M.-G. Alexandru, D. Visinescu, N. Marino, G. Munno, F. Lloretd and M. Julve, *RSC Adv*., 2015, **5**, 95410–95420.

15) Z. Tian, S. Moorthy, H. Xiang, P. Peng, M. You, Q. Zhang, S.-Y. Yang, Y.-L. Zhang, D.-Q. Wu, S. K. Singh and D. Shao, *CrystEngComm*, 2022, **24**, 3928-3937.

16) D. Shao, S. Moorthy, P. Peng, L. Shi, W.-J. Tang, X.-Q. Wei, Z.-J. Wang and S. K. Singh, *Eur. J Inorg. Chem*., 2022, **2022**, e202200354.

17) A. K. Seguin, C. Cruz, K. Villafuerte, D. Páez-Hernández, D. Venegas-Yazigi and V. Paredes-García, *Cryst. Growth Des*., **2023**, 23, 77-86.

18) H. V. P. Hollauer, G. S. de Araújo, G. P. Guedes, H. C. S. Junior, S. Letichevsky, L. Ghivelder, S. Soriano, O. Cambraia and L. B. L. Escobar, *J. Mol. Struct.*, **2024**, 1306, 137811.

19) T. Long, J. Yang, S. Moorthy, D. Shao, S. K. Singh and Y.-Z. Zhang, *Cryst. Growth Des*., **2023**, 23, 2980-2987

20) D. Shao, S. Moorthy, Y.-L. Zhang, J.-P. Shen, J. Yang, S. K. Singh, Y.-Z. Zhang and X.-Y. Wang, *Cryst. Growth Des*., **2024**, 24, 7202-7211.

21) Neese, F. Software Update: The ORCA Program System-Version 5.0. *WIREs Comput. Mol. Sci.* **2022**, 12, e1606.

22) A. D. Becke, *Phys. Rev. A*, **1988**, 38, 3098–3100.

23) F. Weigend and R. Ahlrichs, *Phys. Chem. Chem. Phys*., **2005**, 7, 3297.

24) P.-Å. Malmqvist and B. O. Roos, *Chem. Phys. Lett*., **1989**, 155, 189–194.

25) B. O. Roos, in Methods in Computational Molecular Physics, edited by G. H. F. Diercksen and S. Wilson, Springer Netherlands: Dordrecht, **1983**, pp 161–187.

26) C. Angeli, R. Cimiraglia and J.-P. Malrieu, *J. Chem. Phys*., **2002**, 117, 9138–9153.

27) C. Angeli, R. Cimiraglia, S. Evangelisti, T. Leininger and J.-P. Malrieu, *J. Chem. Phys*., **2001**, 114, 10252–10264.

28) C. Angeli, B. Bories, A. Cavallini and R. Cimiraglia, *J. Chem. Phys*., **2006**, 124, 054108.